Original Article

JCBFM

Journal of Cerebral Blood Flow & Metabolism
2021, Vol. 41(7) 1669–1681

DOI: 10.1177/0271678X20973787
journals.sagepub.com/home/jcbfm
SAGE

Role of endothelial nitric oxide synthase for early brain injury after subarachnoid hemorrhage in mice

Irina J Lenz[1,2], Nikolaus Plesnila[1,2] and Nicole A Terpolilli[1,2,3]

Abstract

The first few hours and days after subarachnoid hemorrhage (SAH) are characterized by cerebral ischemia, spasms of pial arterioles, and a significant reduction of cerebral microperfusion, however, the mechanisms of this early microcirculatory dysfunction are still unknown. Endothelial nitric oxide production is reduced after SAH and exogenous application of NO reduces post-hemorrhagic microvasospasm. Therefore, we hypothesize that the endothelial NO-synthase (eNOS) may be involved in the formation of microvasospasms, microcirculatory dysfunction, and unfavorable outcome after SAH. SAH was induced in male eNOS deficient ($eNOS^{-/-}$) mice by endovascular MCA perforation. Three hours later, the cerebral microcirculation was visualized using *in vivo* 2-photon-microscopy. $eNOS^{-/-}$ mice had more severe SAHs, more severe ischemia, three time more rebleedings, and a massively increased mortality (50 vs. 0%) as compared to wild type (WT) littermate controls. Three hours after SAH $eNOS^{-/-}$ mice had fewer perfused microvessels and 40% more microvasospasms than WT mice. The current study indicates that a proper function of eNOS plays a key role for a favorable outcome after SAH and helps to explain why patients suffering from hypertension or other conditions associated with impaired eNOS function, have a higher risk of unfavorable outcome after SAH.

Keywords

Subarachnoid hemorrhage, early brain injury, endothelial NOS, nitric oxide, microvasospasm

Received 10 June 2020; Revised 27 September 2020; Accepted 15 October 2020

Introduction

Subarachnoid hemorrhage is a subtype of (hemorrhagic) stroke with high mortality and morbidity[1] and survivors of the disease often remain significantly disabled.[2–4] It is increasingly recognized that changes on the level of the cerebral microcirculation occurring within the first few hours and days after aneurysm rupture play an important role for early brain injury (EBI) and unfavorable outcome after SAH.[5–9] Microvasospasms of pial arterioles and a subsequent reduction of parenchymal microperfusion which have been shown to occur as early as three and up to at least 72 hours after experimental SAH and two to three days after SAH in patients significantly contribute to post-hemorrhagic ischemia,[10–15] however, the molecular mechanisms of this process are largely unknown.

Endothelial nitric oxide (NO) is an important mediator of proper cerebro-vascular function.[16] After SAH, NO concentration decreases rapidly[17–20] and replenishing NO bioavailability reduced microvasospasms, improved cerebral perfusion, provided neuroprotection, and improved outcome in experimental models of SAH.[15,21–26] Despite the important role of NO after SAH, the molecular mechanisms of NO depletion are still not well defined. Indirect evidence from experimental studies suggests that the endothelial NO-synthase (eNOS) may be dysfunctional after

[1]Institute for Stroke- and Dementia Research (ISD), Munich University Hospital and Ludwig-Maximilians University, Munich, Germany
[2]Munich Cluster for Systems Neurology (SyNergy), Munich, Germany
[3]Department of Neurosurgery, Munich University Hospital, Munich, Germany

Corresponding author:
Nikolaus Plesnila, Institute for Stroke and Dementia Research, Munich University Hospital and Ludwig-Maximilians University, Feodor-Lynen-Str. 17, 81377 Munich, Germany.
Email: nikolaus.plesnila@med.uni-muenchen.de

SAH[17] and studies in humans demonstrated that genetic polymorphisms decreasing eNOS activity are linked to increased susceptibility for cerebrovascular disease and an increased risk for unfavorable outcome after SAH.[27–29] In the current study we therefore hypothesize that NO produced by eNOS plays a crucial role for post-hemorrhagic microcirculatory dysfunction, early brain injury, and outcome after SAH.

A major obstacle when investigating eNOS is the lack of potent and isoform specific inhibitors and antibodies.[30] Since this is believed to be one of the major causes of heterogeneous results in other brain injury models, such as ischemic stroke or traumatic brain injury, we used a genetic approach, i.e. eNOS deficient mice, to investigate the role of eNOS for outcome and microcirculatory dysfunction after SAH.

Materials and methods

Ethical statement

All procedures performed on animals, group size calculation, and all statistical methods used to analyze in vivo data were reviewed and approved by the Government of Upper Bavaria. The results of the study are reported in accordance with the ARRIVE guidelines.[31] Animal husbandry, health screens and hygiene management checks were performed in accordance with Federation of European Laboratory Animal Science Associations (FELASA) guidelines and recommendations.[32] All surgical procedures and data analysis were performed in a randomized fashion by a researcher blinded to the genotype of the animals. Group allocation was obtained by drawing lots.

Experimental animals

eNOS deficient animals were purchased from Jackson Laboratories (strain #002684, B6.129P2-Nos3tm1Unc/J). In these animals, eNOS knock out is achieved by replacement of 129 base pairs on exon 12 of the eNOS gene by a neomycin cassette which disrupts the calmodulin binding site of the protein and introduces a premature stop codon into the transcripts.[33] Animals were then backcrossed into their C57BL/6J background for more than ten generations. We bred heterozygous mice in order to obtain homozygous and heterozygous offspring as well as littermate controls. Male mice (mean age 8 weeks) with an average bodyweight of 22.5 g were used for experiments.

Anesthesia and monitoring

Anesthesia was induced as previously described[34] under continuous monitoring of end-tidal CO_2 partial pressure, oxygen saturation, heart rate (by oximetry at the hind paw, SpO_2-MSE, Kent Scientific Corporation, Torrington, CT, USA), and body temperature (by a feedback controlled heating pad, FHC Bowdoinham, Bowdoin, ME, USA). Intracranial pressure was measured contralateral to SAH induction using a piezoelectric probe (Codman ICP Express, DePuy Synthes, Umkirch, Germany) placed in the right temporoparietal epidural space as previously described.[35,36] Cerebral blood flow was measured via laser Doppler fluxmetry (Perimed, Järfälla, Sweden) over the ipsilateral MCA territory.[35,36] In chronic experiments, arterial blood pressure was measured non-invasively with a tail-cuff (Kent Scientific, Torrington, CT, USA). After surgery and monitoring, anesthesia was antagonized as previously described[34] and animals were kept in a heating chamber at 34 °C and 40% humidity for up to 24 h in order to prevent hypothermia and dehydration. For intravital microscopy, animals were re-anesthetized and re-intubated 2.5 h after SAH induction. For imaging, an open cranial window (4 x 4 mm) was prepared over the left middle cerebral artery territory 1–1.5 mm rostral to the coronal suture and 2 mm lateral of the midline (Figure 1(a), left and upper right panel). Blood pressure was continuously monitored via a femoral artery catheter. The femoral vein was cannulated for application of the plasma marker fluorescein isothiocyanate (FITC)-dextran (Merck, Darmstadt, Germany).

Induction of subarachnoid hemorrhage

Subarachnoid hemorrhage was induced by the endovascular filament perforation model.[14,15,35] Briefly, a 5-0 monofilament was inserted into the left external carotid artery and advanced towards the circle of Willis under continuous control of cerebral perfusion and intracranial pressure until a sharp increase in intracranial pressure above 60 mmHg and a drop in cerebral perfusion below 20% of baseline was observed as a sign of successful vessel perforation. Animals not fulfilling these criteria were excluded from further analysis. A detailed step-by-step video of the procedure including probe placement can be accessed here: doi: 10.3791/50845). Rebleedings after subarachnoid hemorrhage were defined as secondary increases of ICP by 10 mmHg or more within 10 seconds or less; analysis of secondary ICP events/rebleedings was done automatedly using the intraoperatively recorded data.[36]

2-Photon microscopy

In vivo 2-photon microscopy was performed three hours after induction of subarachnoid hemorrhage every 10 minutes for 90 min as previously described[37–39] using a confocal microscope (LSM 7, Zeiss, Germany) equipped with a Li:Ti laser (Chameleon, Coherent,

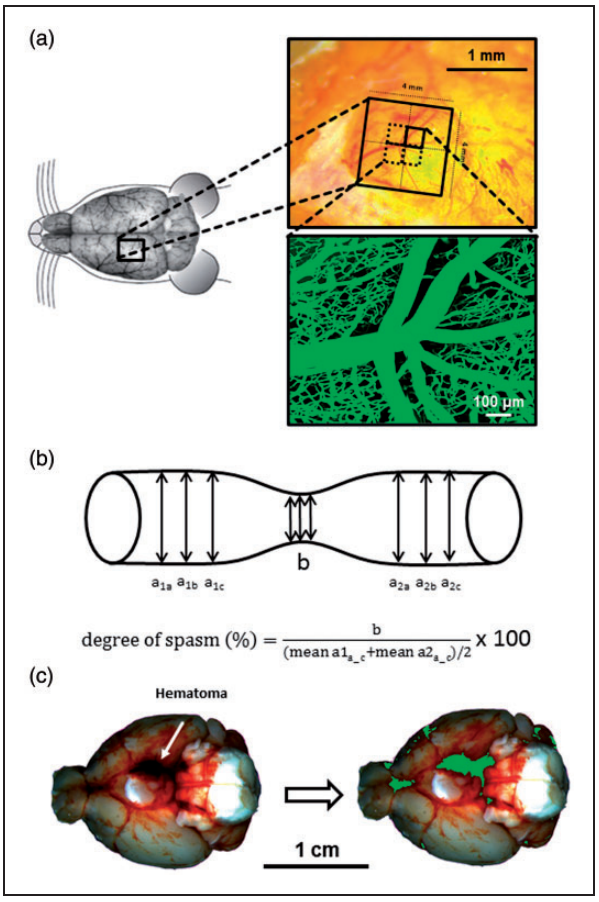

Figure 1. Intravital microscopy - Experimental setup. (a) Schematic overview of cranial window placement for intravital microscopy. (b) Assessment of microvasospams formation and severity. (c) Example of a hematoma at the skull base after SAH (left) and the quantification of hematoma size (green) by an automated algorithm (right).

Santa Clara, CA, USA) and a water immersion objective (20x Plan Apochromat, NA 1.0, Zeiss, Germany) as well as a micromanipulator table for exact placement. Vessels were visualized by i.v. injection of 0.1 ml FITC dextran (0.5% in saline). Three-dimensional images of four adjacent regions of interest (425 x 425 µm each) in the geometrical middle of the exposed area within the craniotomy were acquired up to a depth of 400 µm and then digitally stitched together to form one single image stack of 850 x 850 µm for further analysis (Figure 1(a), lower right panel).

Data analysis

Physiological monitoring was performed at a sample rate of 1 Hz and averaged every 20 seconds. Intravital microscopy data was analyzed using ImageJ version 1.52p. Microvascular constriction and the number of microvasospasms were evaluated as previously described in arterial vessels with diameters ranging from 10 until 80 µm.[14,38] A vessel segment was considered spastic when its diameter was 85% or less than non-constricted vessel segments; spasm severity is given as percent constriction of vessel diameter compared to non-constricted vessel segments (Figure 1(b)). Vessel diameter was assessed for all arterial vessels captured in each scan every 10 –15 µm along the course of the vessel which was traced throughout the 3 D dataset; non-spastic vessel diameters were averaged before and after a spastic segment, the degree of vasospasm was then calculated as described in Figure 1(b). For assessment of total perfused vessel volume all FITC-positive pixels of a stack were summed up and expressed as percentage of all pixels within this stack. All data was analyzed in a blinded fashion by a researcher unaware of the experimental series and the genotype of the animals.

Tail bleeding time

Bleeding time was determined as previously described.[15] Briefly, the distal one millimeter of the tail was amputated and the tail was placed perpendicularly in 37 °C warm saline. The time between incision and stop of bleeding was determined visually.

Determination of hematoma size

All animals were perfused with saline, then brains were carefully removed in a prone position so the blood remained at the brain base. Afterwards, the brains were placed in a prone positions under a stereomicroscope (Leica M205, Zoom: 10.6 x, resolution max. 5251p/mm; Meyer Instruments, Houston, USA) and fotographed at high-resolution. The setup for brain positioning (in a custom made white plastic holder), the position of the lights, and the camera settings were not altered during the whole experiments in order to achieve comparable illumination and image quality. The background of the image obtained was manually extracted using GIMP (The GIMP team, GIMP 2.10.6, https:/www.gimp.org, 1997–2019). Using a purpose made JAVA code written for ImageJ, each image was then automatically analysed and visually crosschecked by a researcher blinded towards experimental group and genotype. The code differentiates between light red blood in the subarachnoid space and the darker red blood representing the basal blood clot as described below:

Color composition of each pixel was analysed and expressed as red (r), green (g), and blue (b) value (each ranging from 0 to 1). If $r+g+b < \text{dark\_threshold}$ (0.235), the pixel was counted as dark red/belonging to the blood clot. The threshold was established by

analyzing images from previous methodological studies using the MCA perforation model and was found to provide a good differentiation between the light red/dark red blood. Pixels exceeding this threshold were quantified as light red, i.e. representing subarachnoid blood, if they fulfilled r>(g + b)/red_sensitivity. Red sensitivity was assumed to be 0 as we were not interested in quantifiying the subarachnoid hematoma, therefore these pixels were not counted. The total number of pixels fulfilling one of two conditions (r + g+b <= dark_threshold or r>(g + b)/red_sensitivity) were then counted and divided by the total number of pixels comprising the brain base. The results of automated analysis was anecdotally crosschecked by a blinded researcher manually marking pixels of the blood clot; results corresponded to a high degree (Figure 1(c)).

Statistical analysis

Sample size calculations were performed before starting the study with the following parameters: alpha error 0.05, beta error 0.2, calculated standard deviation ranged from 15–20% (depending on the parameter investigated), and biologically relevant difference 30%. This calculation also needs to account for mortality that is approximately 30% in 3 days in this model. When interim analysis showed a relevantly increased mortality in eNOS transgenic animals, their number had to be increased in order to achieve the calculated group numbers. In order to guarantee adequate randomization and blinding an equal number of wildtype animals was randomized thereby increasing n in the WT group. Since the resulting sample size was below 25, all data was assumed to be not normally distributed even when it passed normality testing (Kolmogorov-Smirnov method) in order to avoid overestimating a possible effect; therefore, only nonparametrical statistical tests were used for statistical analysis. Two groups were compared with the Mann Whitney rank sum test, multiple groups with Kruskal-Wallis ANOVA on ranks, and repeated measurements with the Friedman test. When indicated, the Dunnet test was performed post-hoc. All calculations were done using a standard statistical software package (SigmaStat 3.0, Jandel Scientific, Erkrath, Germany). Differences between groups were considered to be significant at $p < 0.05$.

Results

After induction of SAH wild type mice displayed a sharp increase in intracranial pressure to around 60 mmHg followed by a recovery to about 20–30 mmHg within a few minutes (Figure 2(a), dark grey circles); no animal had to be excluded due to insufficient primary ICP-increase (<60 mmHg). In heterozygous and homozygous eNOS deficient animals peak ICP values were more than 25 mmHg higher than in wild type mice ($p < 0.001$ vs. WT control, Kruskal-Wallis test, Dunnet's post hoc test). While in heterozygous animals ICP values recovered over time and reached those of wild type mice at the end of the observation period, ICP in homozygous eNOS mice remained significantly elevated (Figure 2(a), light grey and open circles). Cerebral blood flow dropped significantly in all experimental groups immediately after SAH (Figure 2(b)), however, the drop in CBF was

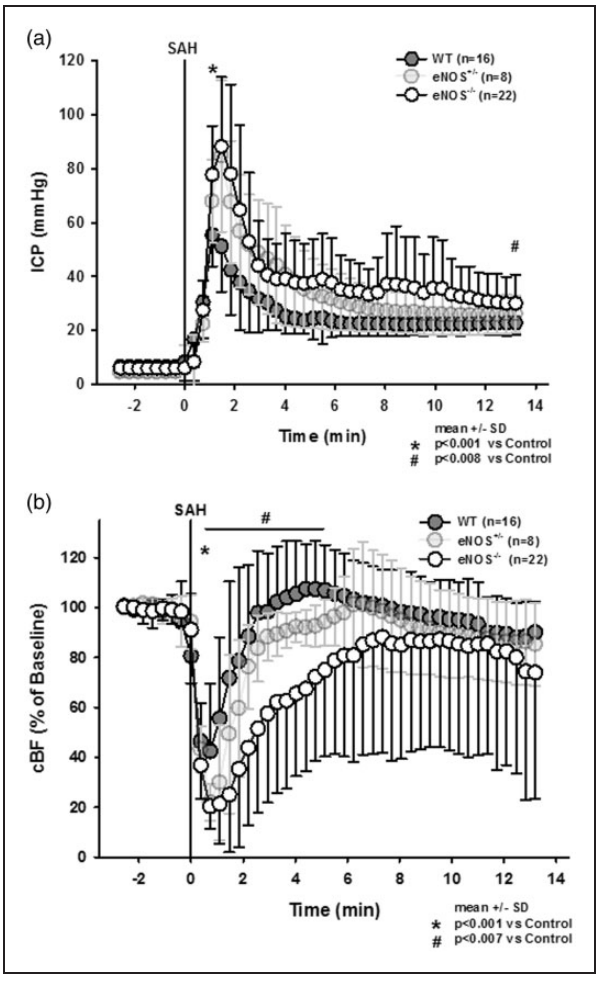

Figure 2. Intracranial pressure and local cerebral blood following subarachnoid hemorrhage. (a) Peak intracranial pressure is significantly and gene-dose-dependently elevated in eNOS deficient mice. After few minutes, ICP drops again but remains significantly elevated in eNOS homozygous animals compared to wild type littermates. (b) Cerebral perfusion drops to lower values in eNOS deficient as compared to wild type mice. While in heterozygous and wild type mice CBF recovers to baseline values within a short time, CBF in homozygous eNOS deficient mice remains significantly impaired.

significantly more pronounced in heterozygous and homozygous eNOS deficient mice. While heterozygous animals recovered to control levels within two minutes, homozygous eNOS mice showed a significantly reduced CBF for more than six minutes (Friedman test).

When ICP recordings from single animals were analyzed, we observed several secondary ICP increases indicating re-bleedings, specifically in eNOS deficient animals. Secondary increases in intracranial pressure accompanied by drops in CBF have been described to be associated with radiologically detectable re-bleeding in CT or angiography[40] and occurred in our previous experimental studies[41,42] where they were associated with worse outcome; while brain edema formation and/or hydrocephalus may account for elevation of ICP, the onset of these phenomenona is not as rapid and it is not as readily reversible, therefore occurrence of re-bleeding events are the most feasible explanation for these occurrences. In order to quantify these observations, an additional cohort of $eNOS^{-/-}$ and corresponding control animals were continuously monitored for up to 180 minutes after SAH. Exemplary traces for a wild type and an $eNOS^{-/-}$ mouse (Figure 3(a)) show no re-bleedings in wild type, but multiple re-bleedings in $eNOS^{-/-}$ mice. Quantification of these events showed a three-fold increase in the number of re-bleedings in $eNOS^{-/-}$ mice as compared to wild type controls or heterozygous eNOS animals (Figure 3(b); $p = 0.004$ vs. WT, $p = 0.022$ vs. $eNOS^{+/-}$, Kruskal-Wallis test, Dunnet's post hoc test).

Re-bleedings may be caused by high blood pressure or by insufficient hemostasis. Since high blood pressure as well as impaired hemostasis were described in $eNOS^{-/-}$ mice,[33,43–45] we analyzed both parameters in our experimental series. When investigating systemic arterial blood pressure in wild type and heterozygous and homozygous eNOS deficient mice, we indeed observed a non-significant trend towards a higher blood pressure of about 10 mmHg in homozygous eNOS deficient mice before and after SAH (Figure 3 (c)). However, the Cushing response was similar in all investigated animals and no blood pressure peaks were observed in eNOS deficient mice. Hence, we were not convinced that this increase in blood pressure is the main reason for the quite impressive re-bleeding phenotype observed in homozygous eNOS deficient mice. Therefore, we investigated hematoma size as a proxy for hemostasis and found a more than twice as large hematoma area in $eNOS^{-/-}$ mice as compared to wild type controls (Figure 4(a); $p < 0.001$, Mann Whitney rank sum test). Since larger hematomas point towards an altered bleeding phenotype in eNOS deficient mice, we assessed the tail bleeding time in our animals.

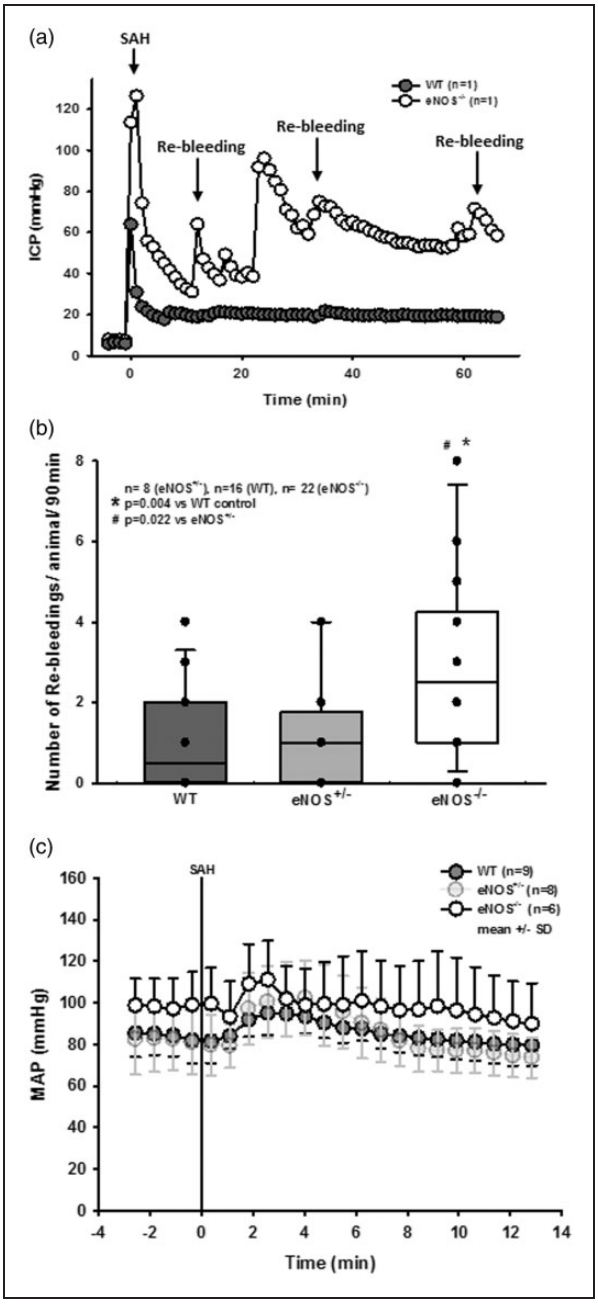

Figure 3. Re-bleeding events. (a) Exemplary ICP traces in single mice show repetitive re-bleedings in an $eNOS^{-/-}$ animal while no such events were observed in a wild type littermate. (b) Quantification reveals a significantly elevated number of re-bleeding events in eNOS homozygous animals compared to wild type and heterozygous mice ($p = 0.004$ and 0.022, respectively). (c) Invasive arterial blood pressure recordings in homozygous (dark grey symbols) and heterozygous (light grey symbols) eNOS deficient mice and wild type littermates before and after SAH. Already before SAH $eNOS^{-/-}$ mice had a slightly increased arterial blood pressure. Within the first four minutes after SAH all three genotypes showed the typical increase in blood pressure due to increased intracranial pressure, the Cushing response. Thereafter, arterial blood pressure returned to baseline levels in all investigated genotypes.

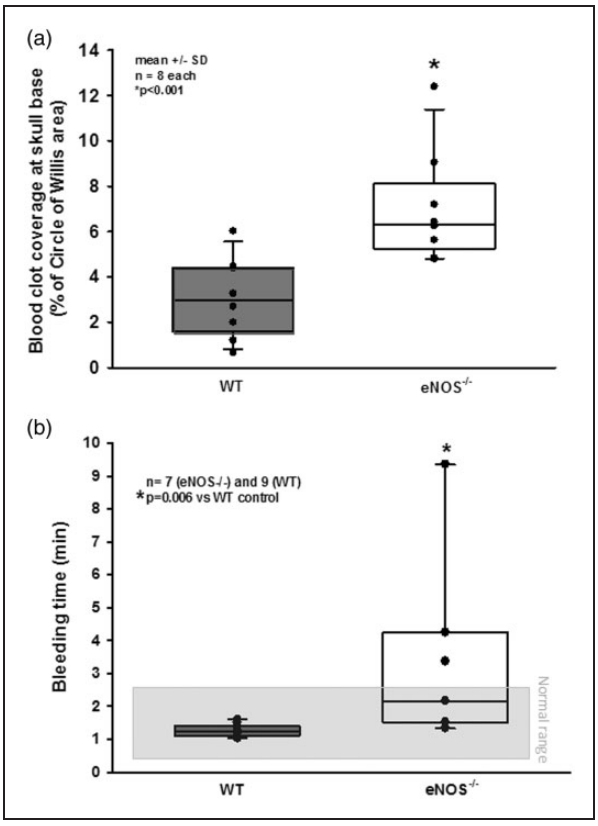

Figure 4. Possible causes for increased SAH severity in eNOS$^{-/-}$ mice. (a) eNOS$^{-/-}$ mice had significantly larger hematomas at the skull base as compared to wild type littermates after SAH. (b) Tail bleeding time was significantly elevated in eNOS deficient animals.

Indeed, eNOS deficient mice had an almost three times longer bleeding time than wild type control mice which had a physiological bleeding time of about one minute. (Figure 4(b); $p = 0.006$, Mann Whitney rank sum test). Bleeding time analysis does not allow for exact differentiation of platelet function and vascular endothelial function as well as the influence of arterial blood pressure. As we did detect a non-significant difference of mean arterial blood pressure between the genotypes, we believe that incomplete hemostasis in combination with (slightly) increased blood pressure is the mechanism behind increased SAH intensity and the re-bleeding phenotype observed in eNOS–/– mice. In order to address the aim of the current study, i.e. the role of eNOS on the cerebral microcirculation after SAH, we subjected wild type and eNOS$^{-/-}$ mice to SAH and observed cerebral blood vessels in vivo by 2-photon microscopy. One wild type and one eNOS mouse had to be excluded due to technical issues during cranial window preparation. Exemplary 2-PM image stacks representing the cerebral microcirculation down to a depth of 400 µm in sham operated mice show a slightly rarefied capillary density in homozygous eNOS mice compared control animals (Figure 5(a), upper panels). This was confirmed by quantification of the perfused vessel volume which showed a significantly decreased vessel density in eNOS$^{-/-}$ mice (Figure 5(b), striped bars; $p < 0.009$, Mann Whitney rank sum test). Of note, this automated evaluation method quantifies the total cerebral microvasculature, i. e. the venous as well as the arterial side. After SAH, there was a significant vessel rarefication in wild type and eNOS$^{-/-}$ animals as compared to control conditions (Figure 5, lower panels and Figure 5(b), solid bars; $p < 0.038$, Kruskal-Wallis test, Dunnet's post hoc test). The decrease in vessel density, however, was more pronounced in eNOS$^{-/-}$ mice. The absolute difference between wild type and eNOS$^{-/-}$ mice was similar to the status before SAH indicating that the loss of endothelial NO production does not aggravate the already existing vascular phenotype in eNOS$^{-/-}$ mice.

For evaluation of micro-arteriolar spasms about 360 vessel segments with an average length of 174 µm were analyzed in wild type and eNOS$^{-/-}$ mice. Following sham surgery very few spasm-like constrictions were observed in wild type mice, while eNOS$^{-/-}$ mice had a more than three-fold higher rate of spontaneous micro-arteriolar spasms (Figure 5(c), striped bars; $p = 0.002$, Mann Whitney rank sum test). Lack of basal production of the vasodilator NO in endothelial cells may well explain this so far unidentified phenotype. After SAH the number of micro-arteriolar spasms almost tripled in wild type mice, while in eNOS$^{-/-}$ mice the number of spasms increased only by about 40%, though from a higher level (Figure 5(c), solid bars; $p = 0.04$, Mann Whitney rank sum test). As already determined in earlier studies,[14,15] micro-arteriolar spasms after SAH occurred predominantly in microvessels with a diameter below 30 µm (Supplemental Figure 1a and b). These data indicate that eNOS deficiency causes a reduction of cerebro-vascular density and the formation of micro-arteriolar spasms already under physiological conditions. SAH worsens this phenotype and may thus cause additional brain damage. This conclusion is supported by the massively elevated mortality in eNOS deficient animals. While none of the 16 investigated wild type animals died after SAH and heterozygous eNOS transgenic mice showed a moderately increased mortality of 25% (2/8 mice), 48% of investigated eNOS$^{-/-}$ mice (12/25) did not survive the first three hours after hemorrhage (Figure 6; $p < 0.001$, Log-Rank test).

Discussion

In the present study, we demonstrate that eNOS-deficient mice have significantly increased morbidity

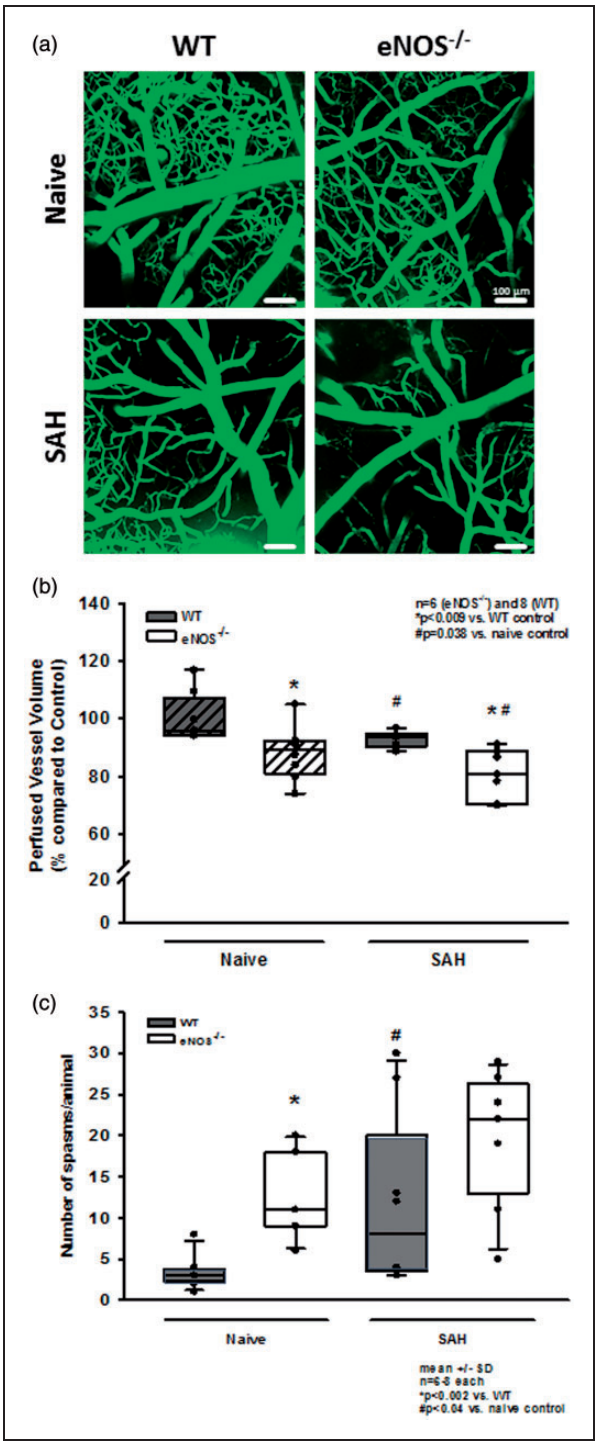

Figure 5. Changes of the cerebral microcirculation after SAH. (a) Exemplary IVM screenshots depicting the cerebral microcirculation in naïve animals (upper panels) and after induction of SAH (lower panels). eNOS deficient mice already show a slight narrowing and rarefication on the capillary level. After SAH, there is (increased) microvascular constriction in both genotypes. (b) Corresponding to the exemplary picture, total perfused vessel volume is slightly but significantly lower in eNOS$^{-/-}$ homozygous animals compared to wild type mice. After SAH, perfused vessel volume is significantly lower in both genotypes, indicating relevant microvascular constriction and – thus – microcirculatory dysfunction. The drop in perfused vessel volume, however, is significantly more pronounced in eNOS$^{-/-}$ than in wt. (c) Microvasospasms occur very rarely under physiological conditions in wild type controls (left side, dark bar). The number of MVS in eNOS$^{-/-}$ is significantly elevated. After SAH, there is significant spasm formation in wt mice (right side of panel). This increase is more pronounced in eNOS$^{-/-}$ mice (striped bars).

and mortality after experimental SAH. Hemorrhage is more severe in eNOS$^{-/-}$ animals as indicated by higher peak ICP values and increased hematoma size; this increased SAH severity is most probably caused by elevated blood pressure and a longer bleeding time found in eNOS transgenic animals. Hence, a more severe SAH is part of the post-hemorrhagic phenotype of eNOS transgenic animals. However, also post-hemorrhagic microcirculatory changes are more pronounced in eNOS$^{-/-}$ mice suggesting an important role of eNOS derived NO for the maintenance of proper microvascular function after SAH.

Interestingly, we also found that eNOS deficient mice have a reduced microvessel density and a significant number of microvasospasms already before SAH. These findings are consistent with the important function of eNOS-derived NO for the maintenance of microvascular stability and vascular tone under physiological conditions. These changes did not result in changes in cerebral blood flow (CBF) since an elevated systemic blood pressure compensated the reduced microperfusion, conclusions consistent with published results of normal CBF in eNOS deficient mice.[46]

Furthermore, the present results demonstrate that SAH leads to a marked deterioration of microcirculatory function which - in combination with the increased hemorrhage severity observed in the present study – results in significantly increased post-hemorrhagic mortality. These findings corroborate the importance of eNOS-derived NO and eNOS-dysfunction for the development of early brain injury after subarachnoid hemorrhage.

Early local depletion of nitric oxide has been identified to play an important role in the development of post-ischemic[47–51] and post-traumatic[52–55] brain damage. While a secondary increase of nitric oxide concentration at later time points – most probably due to activation of inducible NO-synthase has repeatedly been demonstrated to be deleterious in these types of brain injury,[56–61] endothelial NO production by eNOS has consistently been considered neuroprotective.[19,24,49,62–69]

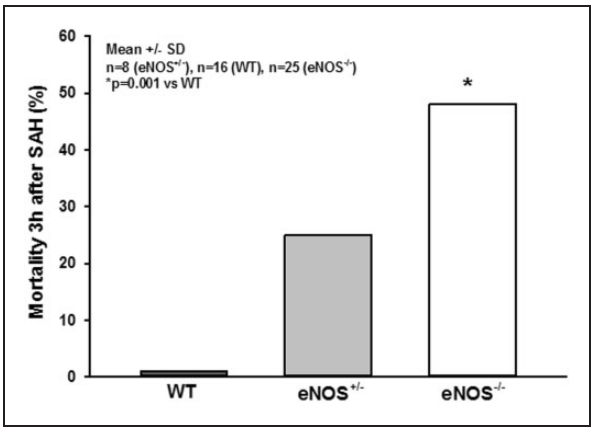

Figure 6. Mortality. While all wild type animals survived the early phase after SAH and heterozygous animals showed a moderately elevated mortality rate of 25%, nearly half of all homozygous eNOS$^{-/-}$ mice died within the first 3 hours after hemorrhage induction.

As for subarachnoid hemorrhage, an early decrease of the NO concentration has been observed in experimental studies[17,18,65,70,71] and in patients.[9,15,72–74] This early NO depletion is linked to microcirculatory dysfunction such as the formation of microvasospasm and microarterial constriction.[15,21,75,76] At later time points the lack of NO has been linked to the formation of (angiographic) vasospasm.[22,67,77,78] Low nitric oxide concentrations also have been shown to facilitate cortical spreading depolarizations[79,80] which may contribute to the development of delayed ischemia after subarachnoid hemorrhage.[79,81,82] It has been speculated that eNOS dysfunction may (partially) be responsible for early NO depletion, especially in brain vessels[19,83–85] and that this may be a cause for early microcirculatory dysfunction.[19] The role of eNOS for maintaining proper microcirculatory function is also supported by the fact that eNOS does not play a significant role in the formation of macrovasospasm after SAH.[56]

The influence of SAH on eNOS activity and expression, however, remained unclear with studies finding no effect of SAH on eNOS activity[86–88] or an increased eNOS activity after experimental SAH.[89] It has also been reported that uncoupling of the homodimeric eNOS complex, which occurs under pathological conditions and has also been reported after experimental subarachnoid hemorrhage, can lead to excess reactive oxygen species formation that aggravates post-ischemic and post-hemorrhagic brain damage.[89] Still, this was found to be accompanied by NO depletion.[89] Hence, the biochemical investigation of eNOS after SAH generated heterogeneous results so far.

In order to overcome the limitations of the biochemical approach, eNOS deficient mice were already previously subjected to experimental SAH.[90] In this previous study, wild type and eNOS deficient mice received an injection of blood into the prechiasmatic cistern and following this procedure less vasospasm of the middle cerebral artery, less microthrombosis, and less apoptotic cell death was observed. These findings were quite surprising, since in all other investigated animal models eNOS deficiency univocally resulted in worse outcome in the context of cerebrovascular pathology.[64,68,71,91–93] One possible explanation may be that the prechiasmatic blood injection model was developed to be able to specifically investigate the effect of blood on larger cerebral arteries located in the subarachnoid space. Hence, the model lacks the clinically relevant feature of vessel perforation and all the subsequent, pathophysiological equally important sequels, e.g. intracranial hypertension, global cerebral ischemia, and microvascular dysfunction. The fact that all relevant changes observed in eNOS deficient mice in the current study are not part of the prechiasmatic blood injection model (increased re-bleeding rate, larger hematoma volume, and impaired microperfusion) may explain the differences between the two studies. One possible drawback of the perforation model is (additional) endothelial injury to extracranial or circle of Willis vessels during advancement of the filament towards the perforation site which deviates from the human pathology where vessel wall injury occurs only at the rupture site; this, however, may incidentally occur in all experimental groups including sham-operation and should therefore not influence our results. Also, focal hypoperfusion or ischemia in the MCA territory may occur immediately after MCA puncture in our model, but is quickly followed by global ischemia when ICP peaks, thereby inducing global hypoperfusion. Of note, hypoperfusion and subsequent ischemia/ischemic damage distal to the vessel rupture site has been described in human SAH[94,95] so this component may be considered a pathophysiological feature which is reproduced by the model. As hemorrhage is more severe in eNOS transgenic animals, the focal ischemia component immediately after rupture may be more pronounced in mutant mice, which may add to the increased SAH pathology observed in eNOS$^{-/-}$ mice.

In previous studies using the same setup as used in the current study,[39,96,97] craniotomy or an open cranial window preparation did not *per se* induce microvascular changes or affect vessel reactivity (neurovascular coupling, CO_2 reactivity); also, there is no evidence of cortical spreading depolarization caused by surgical manipulation unless animals had increased sensitivity towards CSD.[98] While eNOS transgenic animals have not been shown to have increased susceptibility to develop CSDs and while we did not detect any indirect signs

of neurophysiological changes (e. g. reversible waves of hyperperfusion in CBF recording) we cannot exclude that eNOS transgenic animals may react to cranial window preparation with CSDs which may alter or negatively influence cerebral hemodynamics in $eNOS^{-/-}$ mice. As iatrogenic CSDs are more likely to occur when using a traumatic drilling technique utmost care was taken during window preparation; imaging was started 20 minutes after window preparation to minimize possible artifacts. Also, we performed repetitive measurements over a period of up to 110 minutes after surgical manipulation and averaged results. Therefore, we think it highly unlikely that the results obtained in this study are significantly biased by the technique used. Lastly, we would like to mention that the changes observed in the present study were evidenced via a cranial window placed over the left parietal region, ipsilateral to SAH induction at the skull base. After SAH by MCA perforation, blood distributes evenly over the convexity of both hemispheres along perivascular spaces;[36] although we performed a regional analysis we therefore have no reason to believe that the phenomena observed in the present study are limited to the left parietal region.

The present results suggest an important role of endothelial NO production for the pathophysiology of SAH. Chronic lack of endothelial NO, as also observed in patients suffering from hypertension and atherosclerosis, a risk factor for SAH, seems to reduce neurovascular capillary density and to cause arteriolar spasms already under physiological conditions. If SAH occurs on top of this preexisting microvascular pathology, lack of NO causes more severe bleedings due to impaired hemostasis and induces a high rate of rebleedings, one of the most life-threatening complications of SAH. Hence, the findings of the current study may help to explain why patients who suffer from hypertension or other disorders associated with decreased endothelial NO production have a disproportional high rate of unfavorable outcomes after SAH.[99] Therefore, our findings may help to better understand the mechanisms responsible for worse outcome of SAH patients with vascular dysfunction and stress the importance of research efforts directed towards novel therapeutic options to counteract the chronic lack of endothelial NO production in patients at risk for SAH.

Funding

The author(s) disclosed receipt of the following financial support for the research, authorship, and/or publication of this article: This project was supported by the "Fakultätsförderprogramm für Forschung und Lehre" (FöFoLe; project #31/2016) to IJL/NP/NAT by the Medical Faculty of the University of Munich and the Friedrich-Baur-Foundation (NAT, project #63/13) and by the Deutsche Forschungsgemeinschaft (DFG, German Research Foundation) under Germany's Excellence Strategy within the framework of the Munich Cluster for Systems Neurology (EXC 2145 SyNergy – ID 390857198).

Acknowledgements

The authors would like to thank Andreas Lenz, Institute for Communications Engineering, Technical University Munich, for writing the codes for automated assessment of hemorrhage area/perfused blood volume and Janina Biller for technical assistance/animal genotyping.

Declaration of conflicting interests

The author(s) declared no potential conflicts of interest with respect to the research, authorship, and/or publication of this article.

Authors' contributions

IJL performed all experiments, analyzed, and interpreted the data, performed statistical analysis. NAT planned and ideated experiments, analyzed and interpreted the data, performed statistical analysis. NP planned and ideated experiments, interpreted the data. The manuscript was written by IJL, NAT, and NP.

Supplementary material

Supplementary material for this article is available online.

References

1. van Gijn J, Kerr RS and Rinkel GJ. Subarachnoid haemorrhage. *Lancet* 2007; 369: 306–318.
2. Mayer S and Kreiter K. Quality of life after subarachnoid hemorrhage. *J Neurosurg* 2002; 97: 741–742.
3. Schwartz C, Pfefferkorn T, Ebrahimi C, et al. Long-term neurological outcome and quality of life after world federation of neurosurgical societies grades IV and V aneurysmal subarachnoid hemorrhage in an interdisciplinary treatment concept. *Neurosurgery* 2017; 80: 967–974. DOI: 2966486 [pii];10.1093/neuros/nyw138 [doi].
4. Zijlmans JL, Coert BA, van den Berg R, et al. Unfavorable outcome in patients with aneurysmal subarachnoid hemorrhage WFNS grade I. *World Neurosurg* 2018; 118: e217–e222. [pii];10.1016/j.wneu.2018.06.157 [doi].
5. Cahill J, Cahill WJ, Calvert JW, et al. Mechanisms of early brain injury after subarachnoid hemorrhage. *J Cereb Blood Flow Metab* 2006; 26: 1341–1353.
6. Fujii M, Yan J, Rolland WB, et al. Early brain injury, an evolving frontier in subarachnoid hemorrhage research. *Transl Stroke Res* 2013; 4: 432–446.
7. Ostrowski RP, Colohan AR and Zhang JH. Molecular mechanisms of early brain injury after subarachnoid hemorrhage. *Neurol Res* 2006; 28: 399–414.
8. Sehba FA, Hou J, Pluta RM, et al. The importance of early brain injury after subarachnoid hemorrhage. *Prog Neurobiol* 2012; 97: 14–37.

9. Terpolilli NA, Brem C, Bühler D, et al. Are We barking up the wrong vessels? Cerebral microcirculation after subarachnoid hemorrhage. *Stroke* 2015; 46: 3014–3019.
10. Uhl E, Lehmberg J, Steiger H-J, et al. Intraoperative detection of early microvasospasm in patients with subarachnoid hemorrhage by using orthogonal polarization spectral imaging. *Neurosurgery* 2003; 52: 1307–1315.
11. Schubert GA, Seiz M, Hegewald AA, et al. Acute hypoperfusion immediately after subarachnoid hemorrhage: a xenon contrast-enhanced CT study. *J Neurotrauma* 2009; 26: 2225–2231.
12. Sun B-L, Zheng C-B, Yang M-F, et al. Dynamic alterations of cerebral pial microcirculation during experimental subarachnoid hemorrhage. *Cell Mol Neurobiol* 2009; 29: 235–241.
13. Schubert GA, Seiz M, Hegewald AA, et al. Hypoperfusion in the acute phase of subarachnoid hemorrhage. *Acta Neurochir Suppl* 2011; 110: 35–38.
14. Friedrich B, Müller F, Feiler S, et al. Experimental subarachnoid hemorrhage causes early and long-lasting microarterial constriction and microthrombosis: an in-vivo microscopy study. *J Cereb Blood Flow Metab* 2012; 32: 447–455.
15. Terpolilli NA, Feiler S, Dienel A, et al. Nitric oxide inhalation reduces brain damage, prevents mortality, and improves neurological outcome after subarachnoid hemorrhage by resolving early pial microvasospasms. *J Cereb Blood Flow Metab* 2016; 36: 2096–2107.
16. Toda N, Ayajiki K and Okamura T. Cerebral blood flow regulation by nitric oxide: recent advances. *Pharmacol Rev* 2009; 61: 62–97.
17. Sehba FA, Schwartz AY, Chereshnev I, et al. Acute decrease in cerebral nitric oxide levels after subarachnoid hemorrhage. *J Cereb Blood Flow Metab* 2000; 20: 604–611.
18. Schwartz AY, Sehba FA and Bederson JB. Decreased nitric oxide availability contributes to acute cerebral ischemia after subarachnoid hemorrhage. *Neurosurgery* 2000; 47: 208–214.
19. Park KW, Metais C, Dai HB, et al. Microvascular endothelial dysfunction and its mechanism in a rat model of subarachnoid hemorrhage. *Anesth Analg* 2001; 92: 990–996.
20. Hanggi D and Steiger HJ. Nitric oxide in subarachnoid haemorrhage and its therapeutics implications. *Acta Neurochir (Wien)* 2006; 148: 605–613.
21. Sehba FA, Ding WH, Chereshnev I, et al. Effects of S-nitrosoglutathione on acute vasoconstriction and glutamate release after subarachnoid hemorrhage. *Stroke* 1999; 30: 1955–1961.
22. Pluta RM, Afshar JK, Thompson BG, et al. Increased cerebral blood flow but no reversal or prevention of vasospasm in response to L-arginine infusion after subarachnoid hemorrhage. *J Neurosurg* 2000; 92: 121–126.
23. Sun BL, Zhang SM, Xia ZL, et al. L-arginine improves cerebral blood perfusion and vasomotion of microvessels following subarachnoid hemorrhage in rats. *Clin Hemorheol Microcirc* 2003; 29: 391–400.
24. Yang MF, Sun BL, Xia ZL, et al. Alleviation of brain edema by L-arginine following experimental subarachnoid hemorrhage in a rat model. *Clin Hemorheol Microcirc* 2003; 29: 437–443.
25. Sehba FA, Friedrich V Jr, Makonnen G, et al. Acute cerebral vascular injury after subarachnoid hemorrhage and its prevention by administration of a nitric oxide donor. *J Neurosurg* 2007; 106: 321–329.
26. Sehba FA and Friedrich V. Cerebral microvasculature is an early target of subarachnoid hemorrhage. *Acta Neurochir Suppl* 2013; 115: 199–205.
27. Khurana VG, Sohni YR, Mangrum WI, et al. Endothelial nitric oxide synthase gene polymorphisms predict susceptibility to aneurysmal subarachnoid hemorrhage and cerebral vasospasm. *J Cereb Blood Flow Metab* 2004; 24: 291–297.
28. Ko NU, Rajendran P, Kim H, et al. Endothelial nitric oxide synthase polymorphism (-786T->C) and increased risk of angiographic vasospasm after aneurysmal subarachnoid hemorrhage. *Stroke* 2008; 39: 1103–1108.
29. Rosalind Lai PM and Du R. Role of genetic polymorphisms in predicting delayed cerebral ischemia and radiographic vasospasm after aneurysmal subarachnoid hemorrhage: a Meta-Analysis. *World Neurosurg* 2015; 84: 933–941.
30. Poulos TL and Li H. Nitric oxide synthase and structure-based inhibitor design. *Nitric Oxide* 2017; 63: 68–77.
31. Kilkenny C, Browne WJ, Cuthill IC, et al. Improving bioscience research reporting: the ARRIVE guidelines for reporting animal research. *PLoS Biol* 2010; 8: e1000412.
32. Mahler CM, Berard M, Feinstein R, et al. FELASA recommendations for the health monitoring of mouse, rat, hamster, guinea pig and rabbit colonies in breeding and experimental units. *Lab Anim* 2014; 48: 178–192.
33. Shesely EG, Maeda N, Kim HS, et al. Elevated blood pressures in mice lacking endothelial nitric oxide synthase. *Proc Natl Acad Sci U S A* 1996; 93: 13176–13181.
34. Thal SC and Plesnila N. Non-invasive intraoperative monitoring of blood pressure and arterial pCO2 during surgical anesthesia in mice. *J Neurosci Methods* 2007; 159: 261–267.
35. Feiler S, Friedrich B, Scholler K, et al. Standardized induction of subarachnoid hemorrhage in mice by intracranial pressure monitoring. *J Neurosci Methods* 2010; 190: 164–170.
36. Buhler D, Schuller K and Plesnila N. Protocol for the induction of subarachnoid hemorrhage in mice by perforation of the circle of willis with an endovascular filament. *Transl Stroke Res* 2014; 5: 653–659.
37. Schwarzmaier SM, Terpolilli NA, Dienel A, et al. Endothelial nitric oxide synthase mediates arteriolar vasodilatation after traumatic brain injury in mice. *J Neurotrauma* 2015; 32: 731–738.
38. Liu H, Dienel A, Scholler K, et al. Microvasospasms after experimental subarachnoid hemorrhage do not depend on endothelin a receptors. *Stroke* 2018; 49: 693–699.
39. Balbi M, Vega MJ, Lourbopoulos A, et al. Long-term impairment of neurovascular coupling following

experimental subarachnoid hemorrhage. *J Cereb Blood Flow Metab* 2020; 40: 1193–1202.
40. Heuer GG, Smith MJ, Elliott JP, et al. Relationship between intracranial pressure and other clinical variables in patients with aneurysmal subarachnoid hemorrhage. *J Neurosurg* 2004; 101: 408–416.
41. Hockel K, Scholler K, Trabold R, et al. Vasopressin V (1a) receptors mediate posthemorrhagic systemic hypertension thereby determining rebleeding rate and outcome after experimental subarachnoid hemorrhage. *Stroke* 2012; 43: 227–232.
42. Buhler D, Azghandi S, Schuller K, et al. Effect of decompressive craniectomy on outcome following subarachnoid hemorrhage in mice. *Stroke* 2015; 46: 819–826.
43. Huang PL, Huang Z, Mashimo H, et al. Hypertension in mice lacking the gene for endothelial nitric oxide synthase. *Nature* 1995; 377: 239–242.
44. Freedman JE, Sauter R, Battinelli EM, et al. Deficient platelet-derived nitric oxide and enhanced hemostasis in mice lacking the NOSIII gene. *Circ Res* 1999; 84: 1416–1421.
45. Kuhlencordt PJ, Rosel E, Gerszten RE, et al. Role of endothelial nitric oxide synthase in endothelial activation: insights from eNOS knockout endothelial cells. *Am J Physiol Cell Physiol* 2004; 286: C1195–C1202.
46. Atochin DN and Huang PL. Role of endothelial nitric oxide in cerebrovascular regulation. *Curr Pharm Biotechnol* 2011; 12: 1334–1342.
47. Kurose I, Wolf R, Grisham MB, et al. Modulation of ischemia/reperfusion-induced microvascular dysfunction by nitric oxide. *Circ Res* 1994; 74: 376–382.
48. Zhang F, Casey RM, Ross ME, et al. Aminoguanidine ameliorates and L-arginine worsens brain damage from intraluminal middle cerebral artery occlusion. *Stroke* 1996; 27: 317–323.
49. Zhang ZG, Chopp M, Bailey F, et al. Nitric oxide changes in the rat brain after transient middle cerebral artery occlusion. *J Neurol Sci* 1995; 128: 22–27.
50. Uetsuka S, Fujisawa H, Yasuda H, et al. Severe cerebral blood flow reduction inhibits nitric oxide synthesis. *J Neurotrauma* 2002; 19: 1105–1116.
51. Terpolilli NA, Kim SW, Thal SC, et al. Inhalation of nitric oxide prevents ischemic brain damage in experimental stroke by selective dilatation of collateral arterioles. *Circ Res* 2012; 110: 727–738.
52. Cherian L, Goodman JC and Robertson CS. Brain nitric oxide changes after controlled cortical impact injury in rats. *J Neurophysiol* 2000; 83: 2171–2178.
53. Cherian L, Hlatky R and Robertson CS. Comparison of tetrahydrobiopterin and L-arginine on cerebral blood flow after controlled cortical impact injury in rats. *J Neurotrauma* 2004; 21: 1196–1203.
54. Cherian L and Robertson CS. L-arginine and free radical scavengers increase cerebral blood flow and brain tissue nitric oxide concentrations after controlled cortical impact injury in rats. *J Neurotrauma* 2003; 20: 77–85.
55. Terpolilli NA, Kim SW, Thal SC, et al. Inhaled nitric oxide reduces secondary brain damage after traumatic brain injury in mice. *J Cereb Blood Flow Metab* 2013; 33: 311–318.
56. Iadecola C, Zhang F and Xu X. Inhibition of inducible nitric oxide synthase ameliorates cerebral ischemic damage. *Am J Physiol* 1995; 268: R286–R292.
57. Iadecola C, Zhang F, Casey R, et al. Delayed reduction of ischemic brain injury and neurological deficits in mice lacking the inducible nitric oxide synthase gene. *J Neurosci* 1997; 17: 9157–9164.
58. Wada K, Chatzipanteli K, Kraydieh S, et al. Inducible nitric oxide synthase expression after traumatic brain injury and neuroprotection with aminoguanidine treatment in rats. *Neurosurgery* 1998; 43: 1427–1436.
59. Stoffel M, Rinecker M, Plesnila N, et al. Attenuation of secondary lesion growth in the brain after trauma by selective inhibition of the inducible NO-synthase. *Acta Neurochir Suppl* 2000; 76: 357–358.
60. Jafarian-Tehrani M, Louin G, Royo NC, et al. 1400W, a potent selective inducible NOS inhibitor, improves histopathological outcome following traumatic brain injury in rats. *Nitric Oxide* 2005; 12: 61–69.
61. Louin G, Marchand-Verrecchia C, Palmier B, et al. Selective inhibition of inducible nitric oxide synthase reduces neurological deficit but not cerebral edema following traumatic brain injury. *Neuropharmacology* 2006; 50: 182–190.
62. Yamada M, Huang Z, Dalkara T, et al. Endothelial nitric oxide synthase-dependent cerebral blood flow augmentation by L-arginine after chronic statin treatment. *J Cereb Blood Flow Metab* 2000; 20: 709–717.
63. Lo EH, Hara H, Rogowska J, et al. Temporal correlation mapping analysis of the hemodynamic penumbra in mutant mice deficient in endothelial nitric oxide synthase gene expression. *Stroke* 1996; 27: 1381–1385.
64. Huang Z, Huang PL, Ma J, et al. Enlarged infarcts in endothelial nitric oxide synthase knockout mice are attenuated by nitro-L-arginine. *J Cereb Blood Flow Metab* 1996; 16: 981–987.
65. Vellimana AK, Milner E, Azad TD, et al. Endothelial nitric oxide synthase mediates endogenous protection against subarachnoid hemorrhage-induced cerebral vasospasm. *Stroke* 2011; 42: 776–782.
66. Santizo R, Baughman VL and Pelligrino DA. Relative contributions from neuronal and endothelial nitric oxide synthases to regional cerebral blood flow changes during forebrain ischemia in rats. *Neuroreport* 2000; 11: 1549–1553.
67. Pluta RM. Dysfunction of nitric oxide synthases as a cause and therapeutic target in delayed cerebral vasospasm after SAH. *Neurol Res* 2006; 28: 730–737.
68. Hlatky R, Lui H, Cherian L, et al. The role of endothelial nitric oxide synthase in the cerebral hemodynamics after controlled cortical impact injury in mice. *J Neurotrauma* 2003; 20: 995–1006.

69. Berra LV, Carcereri DP, Suzuki H, et al. The role of constitutive and inducible nitric oxide synthase in the human brain after subarachnoid hemorrhage. *J Neurosurg Sci* 2007; 51: 1–9.
70. Neuschmelting V, Marbacher S, Fathi AR, et al. Elevated level of endothelin-1 in cerebrospinal fluid and lack of nitric oxide in basilar arterial plasma associated with cerebral vasospasm after subarachnoid haemorrhage in rabbits. *Acta Neurochir (Wien)* 2009; 151: 795–801.
71. Lundblad C, Grande PO and Bentzer P. Hemodynamic and histological effects of traumatic brain injury in eNOS-deficient mice. *J Neurotrauma* 2009; 26: 1953–1962.
72. Sakowitz OW, Wolfrum S, Sarrafzadeh AS, et al. Relation of cerebral energy metabolism and extracellular nitrite and nitrate concentrations in patients after aneurysmal subarachnoid hemorrhage. *J Cereb Blood Flow Metab* 2001; 21: 1067–1076.
73. Sadamitsu D, Kuroda Y, Nagamitsu T, et al. Cerebrospinal fluid and plasma concentrations of nitric oxide metabolites in postoperative patients with subarachnoid hemorrhage. *Crit Care Med* 2001; 29: 77–79.
74. Durmaz R, Ozkara E, Kanbak G, et al. Nitric oxide level and adenosine deaminase activity in cerebrospinal fluid of patients with subarachnoid hemorrhage. *Turk Neurosurg* 2008; 18: 157–164.
75. Sehba FA and Friedrich V. Early micro vascular changes after subarachnoid hemorrhage. *Acta Neurochir Suppl* 2011; 110: 49–55.
76. Sehba FA, Chereshnev I, Maayani S, et al. Nitric oxide synthase in acute alteration of nitric oxide levels after subarachnoid hemorrhage. *Neurosurgery* 2004; 55: 671–677.
77. Pluta RM and Oldfield EH. Analysis of nitric oxide (NO) in cerebral vasospasm after aneursymal bleeding. *Rev Recent Clin Trials* 2007; 2: 59–67.
78. Fathi AR, Pluta RM, Bakhtian KD, et al. Reversal of cerebral vasospasm via intravenous sodium nitrite after subarachnoid hemorrhage in primates. *J Neurosurg* 2011; 115: 1213–1220.
79. Dreier JP, Korner K, Ebert N, et al. Nitric oxide scavenging by hemoglobin or nitric oxide synthase inhibition by N-nitro-L-arginine induces cortical spreading ischemia when K+ is increased in the subarachnoid space. *J Cereb Blood Flow Metab* 1998; 18: 978–990.
80. Petzold GC, Haack S, von Bohlen Und HO, et al. Nitric oxide modulates spreading depolarization threshold in the human and rodent cortex. *Stroke* 2008; 39: 1292–1299.
81. Bosche B, Graf R, Ernestus RI, et al. Recurrent spreading depolarizations after subarachnoid hemorrhage decreases oxygen availability in human cerebral cortex. *Ann Neurol* 2010; 67: 607–617.
82. Woitzik J, Dreier JP, Hecht N, et al. Delayed cerebral ischemia and spreading depolarization in absence of angiographic vasospasm after subarachnoid hemorrhage. *J Cereb Blood Flow Metab* 2012; 32: 203–212.
83. Hino A, Tokuyama Y, Weir B, et al. Changes in endothelial nitric oxide synthase mRNA during vasospasm after subarachnoid hemorrhage in monkeys. *Neurosurgery* 1996; 39: 562–567.
84. Santhanam AV, Smith LA, Akiyama M, et al. Role of endothelial NO synthase phosphorylation in cerebrovascular protective effect of recombinant erythropoietin during subarachnoid hemorrhage-induced cerebral vasospasm. *Stroke* 2005; 36: 2731–2737.
85. Sehba FA and Bederson JB. Nitric oxide in early brain injury after subarachnoid hemorrhage. *Acta Neurochir Suppl* 2011; 110: 99–103.
86. McGirt MJ, Lynch JR, Parra A, et al. Simvastatin increases endothelial nitric oxide synthase and ameliorates cerebral vasospasm resulting from subarachnoid hemorrhage. *Stroke* 2002; 33: 2950–2956.
87. Sugawara T, Ayer R, Jadhav V, et al. Simvastatin attenuation of cerebral vasospasm after subarachnoid hemorrhage in rats via increased phosphorylation of Akt and endothelial nitric oxide synthase. *J Neurosci Res* 2008; 86: 3635–3643.
88. Osuka K, Watanabe Y, Usuda N, et al. Modification of endothelial nitric oxide synthase through AMPK after experimental subarachnoid hemorrhage. *J Neurotrauma* 2009; 26: 1157–1165.
89. Sabri M, Ai J, Knight B, et al. Uncoupling of endothelial nitric oxide synthase after experimental subarachnoid hemorrhage. *J Cereb Blood Flow Metab* 2011; 31: 190–199.
90. Sabri M, Ai J, Lass E, et al. Genetic elimination of eNOS reduces secondary complications of experimental subarachnoid hemorrhage. *J Cereb Blood Flow Metab* 2013; 33: 1008–1014.
91. Atochin DN, Clark J, Demchenko IT, et al. Rapid cerebral ischemic preconditioning in mice deficient in endothelial and neuronal nitric oxide synthases. *Stroke* 2003; 34: 1299–1303.
92. Atochin DN, Wang A, Liu VW, et al. The phosphorylation state of eNOS modulates vascular reactivity and outcome of cerebral ischemia in vivo. *J Clin Invest* 2007; 117: 1961–1967.
93. Atochin DN and Huang PL. Endothelial nitric oxide synthase transgenic models of endothelial dysfunction. *Pflugers Arch* 2010; 460: 965–974.
94. Rabinstein AA, Weigand S, Atkinson JL, et al. Patterns of cerebral infarction in aneurysmal subarachnoid hemorrhage. *Stroke* 2005; 36: 992–997.
95. Schmidt JM, Rincon F, Fernandez A, et al. Cerebral infarction associated with acute subarachnoid hemorrhage. *Neurocrit Care* 2007; 7: 10–17.
96. Balbi M, Koide M, Wellman GC, et al. Inversion of neurovascular coupling after subarachnoid hemorrhage in vivo. *J Cereb Blood Flow Metab* 2017; 37: 3625–3634.

97. Balbi M, Koide M, Schwarzmaier SM, et al. Acute changes in neurovascular reactivity after subarachnoid hemorrhage in vivo. *J Cereb Blood Flow Metab* 2017; 37: 178–187.
98. van den Maagdenberg AM, Pizzorusso T, Kaja S, et al. High cortical spreading depression susceptibility and migraine-associated symptoms in Ca(v)2.1 S218L mice. *Ann Neurol* 2010; 67: 85–98.
99. Zheng J, Xu R, Liu G, et al. Effect of premorbid hypertension control on outcome of patients with aneurysmal subarachnoid hemorrhage. *Acta Neurochir (Wien)* 2018; 160: 2401–2407.